Biochemical Pharmacology 83 (2012) 207–217

Contents lists available at SciVerse ScienceDirect

Biochemical Pharmacology

journal homepage: www.elsevier.com/locate/biochempharm

Proteasome-based mechanisms of intrinsic and acquired bortezomib resistance in non-small cell lung cancer

Leonie H.A.M. de Wilt [a], Gerrit Jansen [b], Yehuda G. Assaraf [c], Johan van Meerloo [d], Jacqueline Cloos [d], Aaron D. Schimmer [e], Elena T. Chan [f], Christopher J. Kirk [f], Godefridus J. Peters [a], Frank A.E. Kruyt [g,*]

[a] Department of Medical Oncology, VU University Medical Center, Amsterdam, The Netherlands
[b] Department of Rheumatology, VU University Medical Center, Amsterdam, The Netherlands
[c] The Fred Wyszkowski Cancer Research Lab, Department of Biology, Technion-Israel Institute of Technology, Haifa, Israel
[d] Department of Pediatric Oncology/Hematology, VU University Medical Center, Amsterdam, The Netherlands
[e] Princess Margeret Hospital, Ontario Cancer Institute, Toronto, Canada
[f] Onyx Pharmaceuticals, South San Francisco, USA
[g] Department of Medical Oncology, University of Groningen, University Medical Center Groningen, Groningen, The Netherlands

ARTICLE INFO

Article history:
Received 26 August 2011
Accepted 11 October 2011
Available online 18 October 2011

Keywords:
Bortezomib
Resistance
Lung cancer
Mutation
β5 proteasome subunit
Proteasome inhibitors

ABSTRACT

The proteasome inhibitor bortezomib, registered for Multiple Myeloma treatment, is currently explored for activity in solid tumors including non-small cell lung cancer (NSCLC). Here we studied the proteasome-based mechanisms underlying intrinsic and acquired bortezomib resistance in NSCLC cells. Various NSCLC cell lines displayed differential intrinsic sensitivities to bortezomib. High basal chymotrypsin- and caspase-like proteasome activities correlated with bortezomib resistance in these cells. Next, via stepwise selection, acquired bortezomib resistant cells were obtained with 8–70-fold increased resistance. Cross-resistance was found to proteasome inhibitors specifically targeting β-subunits, but not to the novel α-subunit-specific proteasome inhibitor (5AHQ). Consistently, bortezomib-resistant cells required higher bortezomib concentrations to induce G2/M arrest and apoptosis. Interestingly, bortezomib concentration-dependent caspase cleavage, Mcl-1 and NOXA accumulation remained intact in resistant H460 and SW1573 cells, while A549 resistant cells displayed different expression profiles suggesting additional and more protein specific adaptations. Furthermore, bortezomib-resistant cells exhibited increased levels of both constitutive and immuno-β-subunits. Sequence analysis of the bortezomib-binding pocket in the β5-subunit revealed Ala49Thr, Met45Val and Cys52Phe substitutions that were not previously described in solid tumors. Bortezomib-resistant cells displayed reduced catalytic proteasome activities and required higher bortezomib concentrations to achieve comparable inhibition of proteasome activity. Taken together, these findings establish that high basal levels of proteasome activity correlate with intrinsic bortezomib resistance. Furthermore, acquired bortezomib resistance in NSCLC is associated with proteasome subunit overexpression and emergence of mutant β5-subunits that likely compromise bortezomib binding. α-Subunit-specific proteasome inhibitors, however, can efficiently bypass this resistance modality.

1. Introduction

The ubiquitin-proteasome system (UPS) catalyzes the degradation of ubiquitinated intracellular proteins [1–3]. Over the past decades, the role of UPS has proven to be a crucial regulator of cell proliferation and survival by controlling cellular levels of key proteins in these processes [4,5]. Polyubiquitinated proteins are transported to the 26S proteasome for degradation where the 19S cap recognizes, denatures and directs the targeted protein to the catalytic 20S core of the proteasome. The core consists of two outer α-rings and two inner β-rings. Each of the β-rings contains subunits that harbour three proteolytic sites; the caspase-like (β1-subunit), the trypsin-like (β2-subunit) and the chymotrypsin-like activity (β5-subunit) [3]. In vertebrates, an alternative proteasome, the immunoproteasome, can be expressed when cells are exposed to interferon γ (IFNγ). The β-subunits of the proteasome are replaced by immunosubunits; β1i (LMP2), β2i (MECL1) and β5i (LMP7) which are more efficient in regulating antigen processing [6]. Inhibition of the UPS results in perturbation of intracellular protein homeostasis by accumulation of the

* Corresponding author at: Department of Medical Oncology, University of Groningen, University Medical Center Groningen, Hanzeplein 1, 9713 GZ Groningen, The Netherlands. Tel.: +31 50 3615531; fax: +31 50 3614862.
E-mail address: f.a.e.kruyt@umcg.nl (Frank A.E. Kruyt).

0006-2952/$ – see front matter © 2011 Elsevier Inc. All rights reserved.
doi:10.1016/j.bcp.2011.10.009

poly-ubiquitinated proteins, subsequently inducing cellular stress and apoptosis. Interestingly, UPS inhibition appeared to preferentially affect malignant cells reflecting a higher dependence of tumor cells on the UPS [5]. This finding prompted the development of proteasome inhibitors (PIs). Bortezomib (PS-341, Velcade®), a boronic dipeptide which reversibly binds to the β5-subunit and to a lesser extent to the β1-subunit of the proteasome [7,8], was the first to be introduced for the treatment of multiple myeloma (MM) and mantle cell lymphoma [9]. Building on this success of bortezomib, other small molecule PIs were subsequently developed. Carfilzomib (PR-171), an irreversible tetrapeptide epoxyketone PI, exhibits more specificity for the chymotrypsin-like activity (β5-subunit) than other PIs, and appears to have a more favorable toxicity profile [10,11]. In addition, ONX 0912 (formerly PR-047), a tripeptide epoxyketone was also developed, which is an orally available analogue of carfilzomib that retained its selectivity for the chymotrypsin-like activity of the β5-subunit and the immuno-β5 subunit [12,13]. However, for PIs differences in efficacy have been observed in various preclinical models and MM patients related to intrinsic and acquired mechanisms of drug resistance [9,14,15]. Several determinants of resistance to PIs in preclinical models have been investigated such as increased levels of chaperones including Hsp27, which prevent the activation of the unfolded protein response (UPR) in the endoplasmic reticulum and subsequent apoptosis [14,16]. More direct mechanisms of drug resistance have been recently identified at the proteasome level. These studies revealed that acquired bortezomib resistance in leukemia and lymphoma cell lines was due to β5 proteasome subunit overexpression and mutations in the β5-subunit [17–20]. In clinical studies, the efficacy of bortezomib as a single agent in solid tumors appeared to be much lower than in hematological malignancies [21]. Currently tested combinations of bortezomib with other agents conducted in patients with solid tumors, including non-small cell lung cancer (NSCLC), demonstrated as yet little or no improvements in treatment responses over current therapies for NSCLC [22–29]. Nonetheless, in various preclinical solid tumor models, bortezomib in combination with other therapeutics, such as cytotoxic agents and radiotherapy, demonstrated strong antitumor activity [15]. In addition, recently Xue et al. reported efficacy of bortezomib in mice bearing lung tumors with *Kras*$^{LSL\text{-}G12D/wt}$ and p53-deletion [30]. These mice showed tumor regression and prolonged survival after bortezomib treatment. However, prolonged treatment of the originally sensitive lung cancer resulted in bortezomib resistance indicating adaptation and acquired resistance. The molecular mechanisms underlying bortezomib resistance in solid tumors remain largely unexplored. Therefore, we here investigated the intrinsic resistance of NSCLC to bortezomib. In addition, we established acquired bortezomib resistance in a panel of NSCLC cell lines in order to explore the mechanisms of acquired bortezomib resistance while focusing on proteasome-dependent mechanisms.

2. Materials and methods

2.1. Cell culture and chemicals

The human NSCLC H460, A549 and SW1573 cell lines were obtained from the American Type Culture Collection (Manassas, VA, USA). H460 and A549 cells were grown in RPMI-1640 (Lonza, Verviers, Belgium) and SW1573 in DMEM (Lonza, Verviers, Belgium). Medium was supplemented with 10% fetal bovine serum (Greiner Bio-One, Frinckenhausen, Germany) and 100 units/ml penicillin/streptomycin (Lonza, Verviers, Belgium). Cells were grown at 37 °C in a humidified atmosphere of 5% CO_2.

Bortezomib resistant cells were established through a gradual increase in the concentrations of bortezomib for at least 6 months, from 5 nM bortezomib to 80 to 200 nM for H460, 40 to 100 nM for A549 as well as 30 to 150 nM for SW1573, thereby yielding resistant cells named H460BTZR$_{80}$, H460BTZR$_{200}$, A549BTZR$_{40}$, A549BTZR$_{100}$, SW1573BTZR$_{30}$ and SW1573BTZR$_{150}$. Bortezomib resistant cells were cultured in bortezomib-free medium for at least 72 h before initiation of experiments to exclude interference of the selective bortezomib concentrations.

2.2. Reagents and antibodies

Bortezomib (Velcade®) was obtained from Millennium Pharmaceuticals Inc. (Cambridge, MA, U.S.A.) MG132 was purchased from Calbiochem/Merck (Nottingham, UK) and the cytotoxic peptide 4A6 was synthesized as described previously [31]. The proteasome inhibitor 5-amino-8-hydroxyquinoline (5AHQ) was identified through a screen of a chemical library based on quinoline pharmacophore [32]. Carfilzomib[11], ONX 0912 (formerly PR-047) [13] and ONX 0914 (formerly PR-957) [33] were made available by Onyx Inc. (San Francisco, CA, U.S.A.). Stock solutions of 10 mM for each drug were prepared by dissolving in dimethylsulfoxide (DMSO). Following storage at −20 °C, working solutions were prepared by diluting in medium.

Primary antibodies used for PRO-CISE were α-β5 (1:5000); α-β1 (1:2000); α-β2 (1:3000); α-LMP7, α-LMP2 (1:2000) (Biomol, PA, U.S.A.); α-MECL1 (1:1000) (Santa Cruz Biotechnology, Heidelberg, Germany) diluted in ELISA Buffer (PBS pH 7.4, 1% BSA (w/v), 0.1% Tween-20 (v/v)). Secondary antibodies for β5 (1:2000); for β1 and β2 (1:2000); for LMP7 and LMP2 (1:5000); for MECL1 (1:5000) were obtained form Jackson ImmunoResearch, Suffolk, UK and diluted in ELISA Buffer.

For Western Blot and Native Gel electrophoresis primary antibodies included mouse monoclonal antibody to Ub(P4D1) (Santa Cruz Biotechnology, Heidelberg, Germany), mouse monoclonal anti-β1, anti-β2, and anti-α7 subunit, rabbit-polyclonal anti-β5 subunit (Biomol, PA, USA), rabbit polyclonal anti-caspase-9 (Human specific), anti-cleaved caspase-9 (D330) (Human specific), anti-caspase-3, anti-cleaved caspase-3 (Asp175), anti-PARP, anti-FLIP, anti-Mcl-1 and anti-BID (Cell Signalling Technology, Danvers, USA) mouse monoclonal anti-NOXA (Merck KGaA, Darmstadt, Germany) and anti-β-actin (Sigma–Aldrich Chemicals, Zwijndrecht, The Netherlands) were diluted 1:1000 or 1:10,000 for anti-β-actin in InfraRedDye blocking buffer (Rockland inc., Pennsylvania, USA) 1:1 diluted with PBS-T (PBS with 0.05% Tween-20). Secondary antibodies used were goat-a-mouse-InfraRedDye (1:10,000, 800CW;#926-32210 and 680;#926-32220, Westburg, Leusden, The Netherlands) or goat-a-rabbit-InfraRedDye (800CW;926-32211 and 680;#926-32221, Westburg, Leusden, The Netherlands).

2.3. Growth inhibition assay

Drug toxicity in cells was determined using the MTT (3-[4,5-dimethylthiazol-2-yl]-2,5-diphenyl tetrazolium bromide, Sigma–Aldrich Chemicals, Zwijndrecht, The Netherlands) assay as described previously [34]. Cells were seeded in 96-wells plates (Greiner Bio-one, Frickenhausen, Germany) at 5000 cells/well. After 24 h enabling attachment, cells were exposed to increasing concentrations of the proteasome inhibitors for 72 h. Thereafter, cells were incubated for 1 h with 50 μl of 1 mg/ml MTT solution, followed by addition of 150 μl DMSO. Optical density was measured at 540 nm. IC_{50} values were defined as the concentrations that correspond to a reduction of cell growth by 50% when compared to values of untreated control cells and depicted as means ± SEM.

2.4. Flow cytometric analysis of cell cycle distribution

Cell cycle analysis and cell death measurements were performed as described previously [35]. Briefly, cells were harvested after 24 or 48 h exposure to several concentration of bortezomib and centrifuged for 5 min at 1200 rpm. Subsequently cells were stained with propidium iodide buffer (0.1 mg/ml propidium iodide, 0.1% RNase A) in the dark on ice. DNA content was analyzed by fluorescence activated cell sorting (FACS) analysis (Becton Dickinson, immunocytometry Systems, San Jose, CA, USA) with an acquisition of 10,000 events. Cell death was determined by the sub-G_1 peak.

2.5. Proteasome activity assay in intact cells

To measure the chymotrypsin-like, trypsin-like and caspase-like proteolytic activities of the proteasome in intact cells we used the Proteasome-Glo™ Chymotrypsin-like, Trypsin-like and Caspase-like Cell-Based Assays (Promega, Madison, WI, U.S.A.) according to manufacturers instructions. Briefly, 5000 cells were seeded in white 96 wells plates with a transparent bottom. For the exploration of proteasome inhibition, cells were exposed to a range of bortezomib concentrations for 3 h. Substrates for the chymotrypsin-like, trypsin-like and caspase-like activities (Suc-LLVY-aminoluciferin, Z-LRR-aminoluciferin and Z-nLPnlD-aminoluciferin, respectively) were dissolved in Proteasome-Glo™ Cell-Based Reagent and added on intact cells. After 10 min of incubation luminescence was measured with a Tecan Infinite® 200. The activity was corrected for the amount of cells as was measured by absorbance of the cells after a MTT assay.

2.6. Western blot analysis

Western blot analysis was performed as described previously [36]. Briefly, protein samples were separated by SDS PAGE on 8–15% polyacrylamide gels, transferred onto a PVDF membrane (Millipore, Amsterdam, The Netherlands), and blocked in Infra-RedDye blocking buffer. The membrane was probed with the indicated primary antibodies (overnight at 4 °C), followed by 1 h incubation with the indicated secondary antibodies. Fluorescent proteins were detected by an Odyssey Infrared Imager (LI-COR Biosciences, Lincoln, Nebraska U.S.A.), 84 μm resolution, 0 mm offset and with high quality.

2.7. Proteasome subunit determination with the ProCISE assay

The ProCISE (proteasome constitutive/immunoproteasome subunit enzyme linked generated and immunosorbent) assay was performed on untreated cell lysates as was previously described [37]. Luminescence was measured using a GENios-Basic plate reader (Tecan Austria, GmBH). Data was statistically analyzed with XLfit Excel Add-In (ID Business Solutions Limited).

2.8. DNA sequence analysis

Sequence analysis of the *PSMB5* gene was performed as described previously [19]. Briefly, DNA was isolated from H460/H460BTZR$_{80}$/H460BTZR$_{200}$, A549/A549BTZR$_{40}$/A549 BTZR$_{100}$ and SW1573/SW1573BTZR$_{30}$/SW1573BTZR$_{150}$ cells using a Qia amp DNA blood mini kit (Qiagen, Valencia, CA, U.S.A.). DNA was used for amplification of the second exon of the β5 proteasome subunit by PCR (forward: TTCCGCCATGGAGTCATA, reverse: GTTGGCAAG-CAGTTTGGA). PCR products were sequenced with the dideoxy chain-termination method using ABI Prism TM BigDye Termination and an autosequencer ABI Prism Genetic Analyser 3100 automatic DNA sequencer (Perkin Elmer, Foster City, CA, U.S.A.).

2.9. Native gel electrophoresis

Detection of core particles of the proteasome and proteasome activity by native gel electrophoresis was performed as described previously [38]. In brief, 5×10^6 cells were lysed in 300 μl lysis buffer (50 mM Tris–HCL (pH 8.0), 5 mM $MgCl_2$, 0.5 mM EDTA, 1 mM ATP) and mixed with an equal volume of acid washed glass beads (Sigma–Aldrich Chemicals, Zwijndrecht, The Netherlands). Samples were loaded on a 3.5% gel (90 mM Tris base, 90 mM boric acid, 5 mM $MgCl_2$, 0.5 mM EDTA, 1 mM ATP-$MgCl_2$, 0.1% APS, 0.1% Temed). After separation of the proteins, gels were either used to detect proteasome subunits by Western blot analysis or proteasome activity with the use of the suc-Leu-Leu-Val-Tyr-amc (suc-LLVY-amc) substrate (Enzo Life Sciences, PA, U.S.A.).

2.10. P-glycoprotein activity

P-glycoprotein functional activity was determined as described previously [39,40]. Briefly, 150,000 cells were collected in 500 μl medium and incubated for 1 h at 37 °C in the presence of a fluorescent substrate, Syto16 (1 nM) (Invitrogen, Breda, The Netherlands). After incubation cells were exposed to P-glycoprotein inhibitor Reversin-121 (P121, 10 μM) (Alexis Benelux, Breda, The Netherlands) for 1 h. Cells were washed twice with ice cold PBS supplemented with 0.1% bovine serum albumin (BSA). Mean fluorescence was determined by FACS analysis. P-glycoprotein activity was determined by the ratio of the mean fluorescence of the cells treated with P121-control cells and the mean fluorescence of the cells treated without P121-control cells.

2.11. Statistical analysis

Data were analyzed by the student's *t*-test. A Pearson correlation test was used to determine correlations between variables. *P*-values < 0.05 were considered statistically significant. Statistical analysis was performed using GraphPad Prism5.

3. Results

3.1. Intrinsic resistance to bortezomib correlates with elevated basal levels of cellular proteasome activity

Human NSCLC cell lines H460, A549 and SW1573 were first tested for their sensitivity to bortezomib using the colorimetric MTT assay. Dose-response curves for bortezomib-induced growth inhibition revealed differential intrinsic sensitivity to bortezomib with IC_{50} values of 12.6, 8.7 and 1.7 nM for H460, A549 and SW1573, respectively. We next determined proteasome activity in intact cells of these cell lines; when compared to bortezomib-sensitive SW1573 cells, chymotrypsin- and caspase-like activities were 3- and 4.5-fold higher ($P < 0.05$) in the inherently resistant H460 cell line (Fig. 1A). A549 cells had intermediate basal chymotrypsin- and caspase-like activities with parallel intermediate levels of intrinsic resistance to bortezomib. Statistical analysis using a Pearson-test revealed a correlation between high basal chymotrypsin- and caspase-like activities and inherent bortezomib resistance; $R^2 = 0.99$, $P < 0.05$. Noteworthy, no differences were detected in trypsin-like activity that resides in the β2-subunit of the proteasome which is not targeted by bortezomib. Furthermore, determination of the proteasome subunit expression levels by ProCISE, after normalization for protein content, revealed no relationship with proteasome activities measured in these cells (Fig. 1B). Noteworthy, up to 3-fold higher protein levels of the immuno-proteasome subunits β1 and β5 were found in H460 cells compared to A549 and SW1573 cells. Taken together, high basal levels of chymotrypsin- and caspase-like proteasome activities

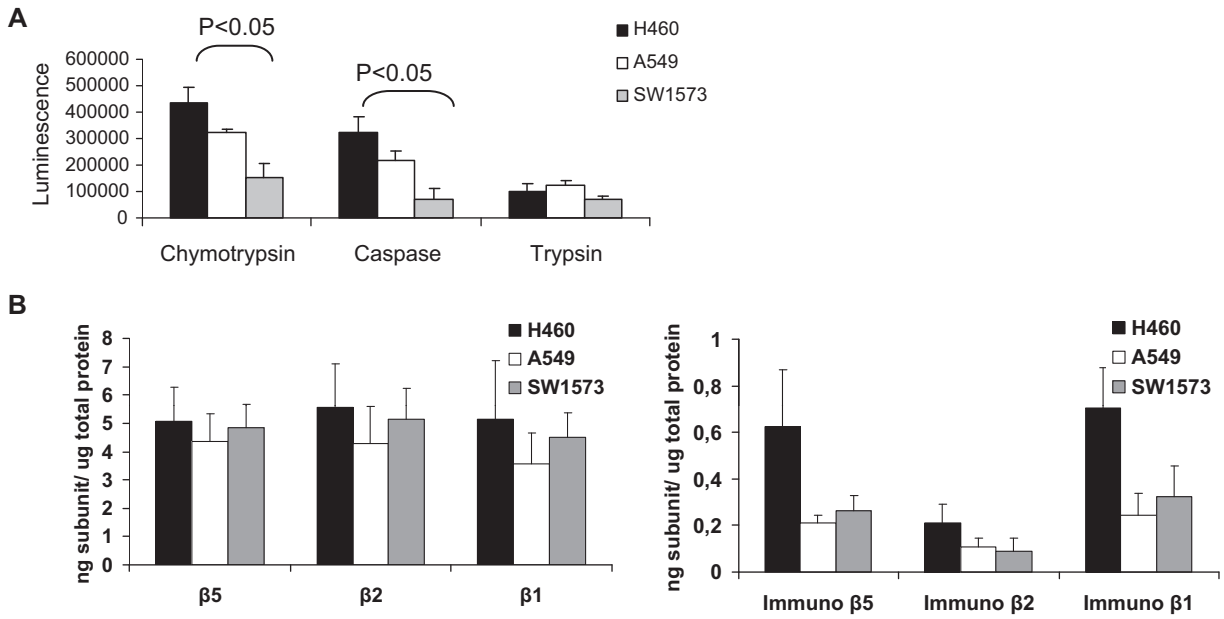

Fig. 1. Intrinsic bortezomib resistance is correlated to higher basal proteasome activities.
(A) Basal proteasome activities demonstrate a significant ($p < 0.05$) higher chymotrypsin- and caspase-like activity in H460 when compared to SW1573. (B) Proteasome subunit levels determined by ProCISE show comparable β-subunits levels and higher immuno proteasome β5 and β1 in H460 cells. Results represent the mean (±SEM) of at least 3 experiments.

correlated with intrinsic bortezomib resistance in these NSCLC cell lines.

3.2. Establishment of NSCLC cell lines with acquired resistance to bortezomib

To investigate the mechanisms underlying acquisition of bortezomib resistance in lung cancer cells, we established a model for acquired bortezomib resistance in NSCLC cells by exposing parental H460, A549 and SW1573 cells to gradually increasing concentrations of bortezomib for at least 6 months. The resulting bortezomib-resistant cell lines were named H460BTZR$_{80}$, H460BTZR$_{200}$, A549BTZR$_{40}$, A549BTZR$_{100}$, SW1573BTZR$_{30}$ and SW1573BTZR$_{150}$, according to the highest selective concentration applied. Dose-response curves of bortezomib-induced growth inhibition revealed resistance of 14- and 22-fold (IC_{50}: 173 and 276 nM) for H460BTZR$_{80}$ and H460BTZR$_{200}$, 8- and 19-fold (IC_{50}: 70 and 167 nM) for A549BTZR$_{40}$ and A549BTZR$_{100}$ and an 18- and 70-fold (IC_{50}: 30 and 119 nM) for SW1573BTZR$_{30}$ and SW1573BTZR$_{150}$, respectively, when compared to their parental counterparts (Fig. 2A). To determine whether or not acquired bortezomib resistance is a stable phenotype, H460BTZR$_{80}$, A549BTZR$_{40}$ and SW1573BTZR$_{30}$ cells were cultured in drug-free medium for 2 months. The drug resistance phenotype was retained, hence indicating that these cell lines harboured a stable bortezomib-resistance phenotype (data not shown). In addition, all bortezomib-resistant cell lines retained parental growth rates as measured with MTT assays (data not shown).

3.3. Status of ubiquitination, cell cycle and cell death in bortezomib-resistant cells

The accumulation of ubiquitinated proteins is a hallmark of proteasome inhibition. A clear alteration in the accumulation of ubiquitinated proteins was observed when cells were incubated for 24 h with bortezomib concentrations ranging from the selective concentrations of the bortezomib-resistant cells and higher (Fig. 2B and Supplementary Fig. 1). A marked accumulation of ubiquitinated proteins was already detectable in parental H460 cells after treatment with 80 nM bortezomib, whereas much higher concentrations were required to obtain similar levels of accumulation of ubiquitinated proteins in H460BTZR$_{80}$ and H460BTZR$_{200}$. Comparable results were obtained with A549, SW1573 cells and their bortezomib-resistant sublines. Furthermore, in line with previous findings [41], bortezomib induced a G2/M cell cycle arrest and cell death in NSCLC cells (Fig. 2C and D). After 24 and 48 h, exposure to 80 nM bortezomib in H460 cells resulted in a marked increase in G2/M arrest and cell death. In H460BTZR$_{80}$ and H460BTZR$_{200}$ high concentrations of 500 nM bortezomib or more were required to achieve a G2/M arrest and cell death. Similar findings were obtained with A549 and SW1573 cells and their bortezomib-resistant counterparts (Supplementary Fig. 2). A lower level of cell death was detected in bortezomib-resistant cells even at equitoxic bortezomib concentrations (Fig. 2D).

In addition, after 48 h exposure to various concentrations of bortezomib, a marked reduction of full length caspase 9, caspase 3 and PARP was found along with the emergence of cleaved products in parental cells; in the bortezomib-resistant counterparts of H460 and SW1573 higher concentrations of bortezomib were required to reach similar effects (Supplementary Fig. 3). In A549BTZR$_{40}$ and parental cells differences in bortezomib dose-dependent caspase cleavage were less pronounced. Furthermore, expression analysis of several pro- and anti-apoptotic proteins revealed that in H460 and SW1573 bortezomib-resistant cells basal Mcl-1 and Noxa expression, known substrates for proteasomal degradation, was unaltered and their bortezomib-induced accumulation remained intact (Supplementary Fig. 4). A549BTZR$_{40}$ cells, however, displayed already enhanced Mcl-1 and Noxa levels that were not further increased upon bortezomib exposure indicating aberrations in their proteasomal turnover. In contrast, the expression of some other apoptosis regulatory proteins that are not direct substrates of the proteasome, such as c-FLIP and Bid was not altered in this cell panel.

Overall, bortezomib-resistant NSCLC cells retained the ability to accumulate ubiquitinated proteins, induce G2/M arrest and

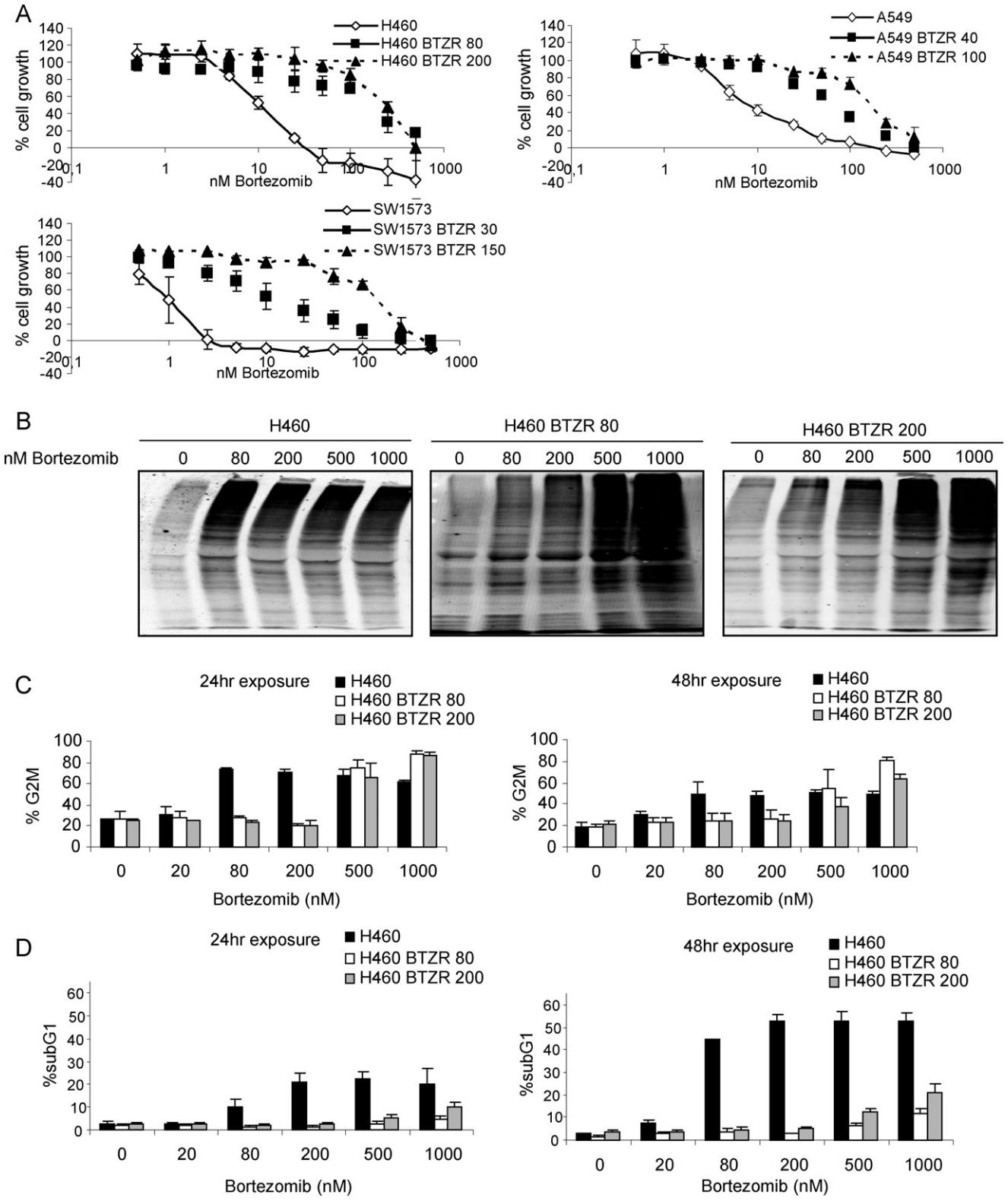

Fig. 2. Bortezomib resistant cells demonstrate diminished accumulation of ubiquitinated proteins, G2M arrest and cell death.
(A) Bortezomib-induced growth inhibition in parental and derived bortezomib resistant cells determined by MTT assay after exposure to bortezomib for 72 h. (B) Western bots showing accumulation of ubiquitinated proteins in H460, H460BTZR$_{80}$ and H460BTZR$_{200}$ after 24 h exposure to different concentrations of bortezomib. (C) and (D) Cell cycle and subG1 (apoptosis) analysis on propidium iodide stained cells treated with increasing bortezomib concentrations for 24 and 48 h. Results represent the mean (±SEM) of at least 3 experiments.

undergo apoptosis, albeit exposure to significantly higher bortezomib concentrations (2.5–6 fold) was required to obtain these effects. Furthermore, higher bortezomib concentrations than the equitoxic concentrations were required to provoke cell death in bortezomib-resistant cells. Caspase activation differed correspondingly in H460 and SW1573, but surprisingly not in A549 bortezomib resistant cells. The degradation and accumulation properties of apoptosis regulatory proteins Mcl-1 and Noxa were

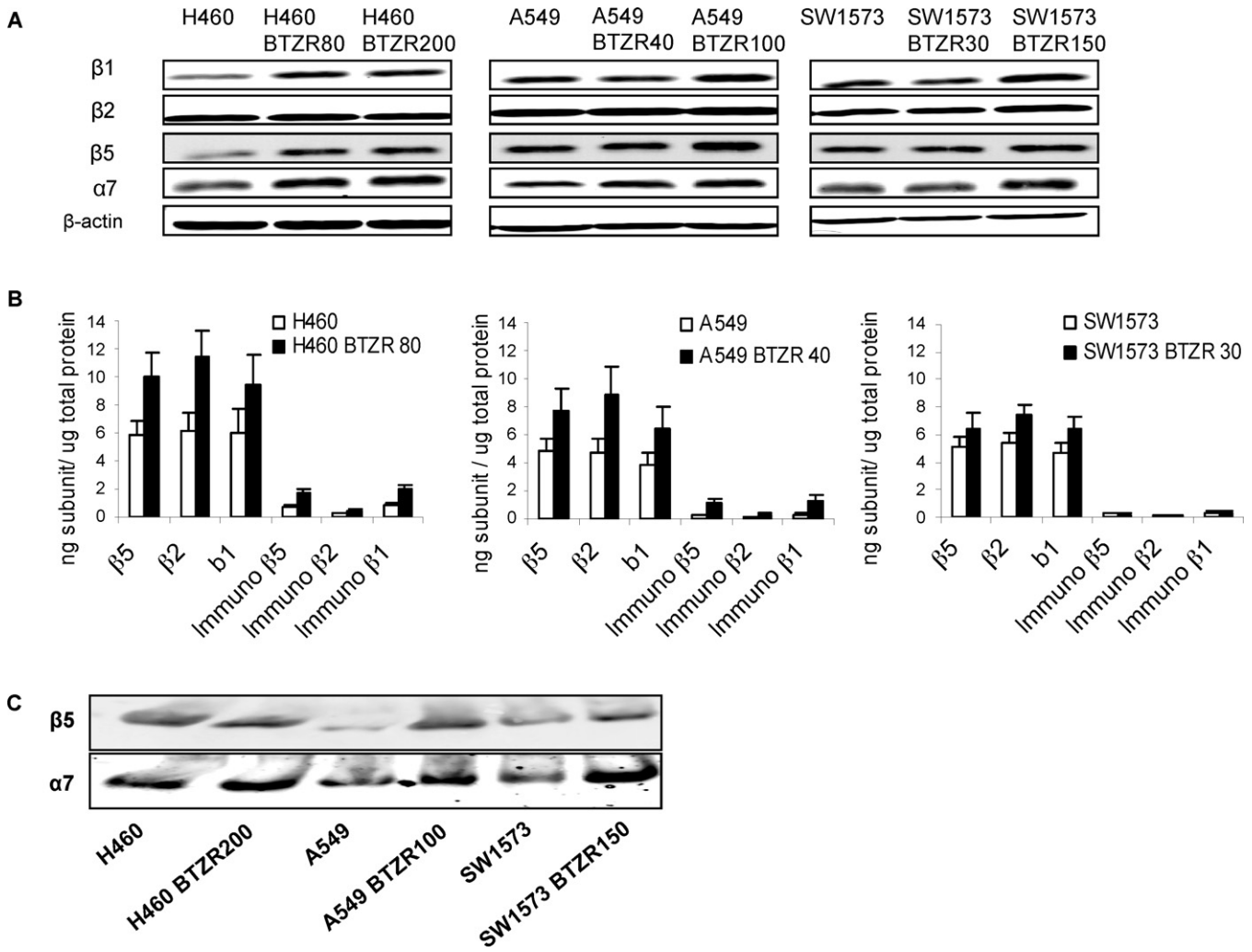

Fig. 3. Increased protein expression levels of the proteasome subunits in the bortezomib resistant cells.
(A) Western blot analysis of the β-subunits demonstrates higher levels for β1, β5 and α7 in the bortezomib resistant variants. β-actin was used as a loading control. (B) Constitutive and immuno-β-subunits expression (ng) analyzed by ProCISE in lysates of parental and bortezomib-resistant cells, showing elevated levels in resistant cells. (C) Native gel electrophoresis detected increased levels of β5 and α7 subunits in acquired bortezomib-resistant cells.

not altered in H460 and SW1573 parental and resistant cells. In A549 bortezomib resistant cells, however, the turnover characteristics of these proteins are different and may reflect additional, yet unknown protein specific alterations in proteasome-based mechanisms of resistance.

3.4. Increased protein levels of proteasome-subunits in bortezomib-resistant cells

To further assess the role of the proteasome subunits in bortezomib-resistance, we determined the expression levels of the β-subunits by Western blot analysis and ProCISE (Fig. 3A and B). Overall, in the drug-resistant derivatives, somewhat higher levels of subunit expression were seen when compared to parental cells. These increases ranged from 1.3 to 1.8-fold for β5, 1.5 to 1.8-fold for β2 and a 1.3 to 1.6-fold for β1 (Fig. 3B). Furthermore, Western blot analysis also revealed increased levels of proteasome subunit α7 (Fig. 3A). Intriguingly, the expression of the immuno-proteasome subunits was enhanced in the H460 and A549 bortezomib-resistant variants, but not in bortezomib-resistant SW1573 cells. The most dramatic increase was observed in A549BTZR$_{40}$ cells with a 5-, 3.5- and 5-fold increase in immuno-β1, immuno-β2 and immuno-β5 subunits, respectively (Fig. 3B). To determine whether increased levels of the proteasome subunits were associated to the 20S core of proteasome, we determined the expression levels of β5 and α7 by native gel electrophoresis (Fig. 3C). Results clearly demonstrate increased levels of the β5 and α7 subunits in the proteasome of bortezomib-resistant cells when compared to their parental cells, indicating an overall increase of proteasome formation in bortezomib-resistant cells.

3.5. Bortezomib-induced inhibition of proteasome activity in parental and bortezomib-resistant cells

We next determined the inhibition of proteasome activities in intact bortezomib-resistant NSCLC cells. After 3 h exposure to various bortezomib concentrations, similar levels of inhibition of the chymotrypsin-like and caspase-like activities were observed in parental cells (Fig. 4A, left panel). For 80% reduction of the chymotrypsin-like and caspase-like activities, bortezomib concentrations ranging from 12 to 16 nM and 61 to 122 nM, respectively, were required. The trypsin-like activity was only slightly suppressed by high bortezomib concentrations of ≥100 nM, whereas low concentrations of 1–25 nM resulted in an increase of trypsin-like activity of up to 50%. In the bortezomib-resistant cells a 1.5–2.5-fold higher bortezomib concentration was required to obtain similar inhibition of chymotrypsin- and

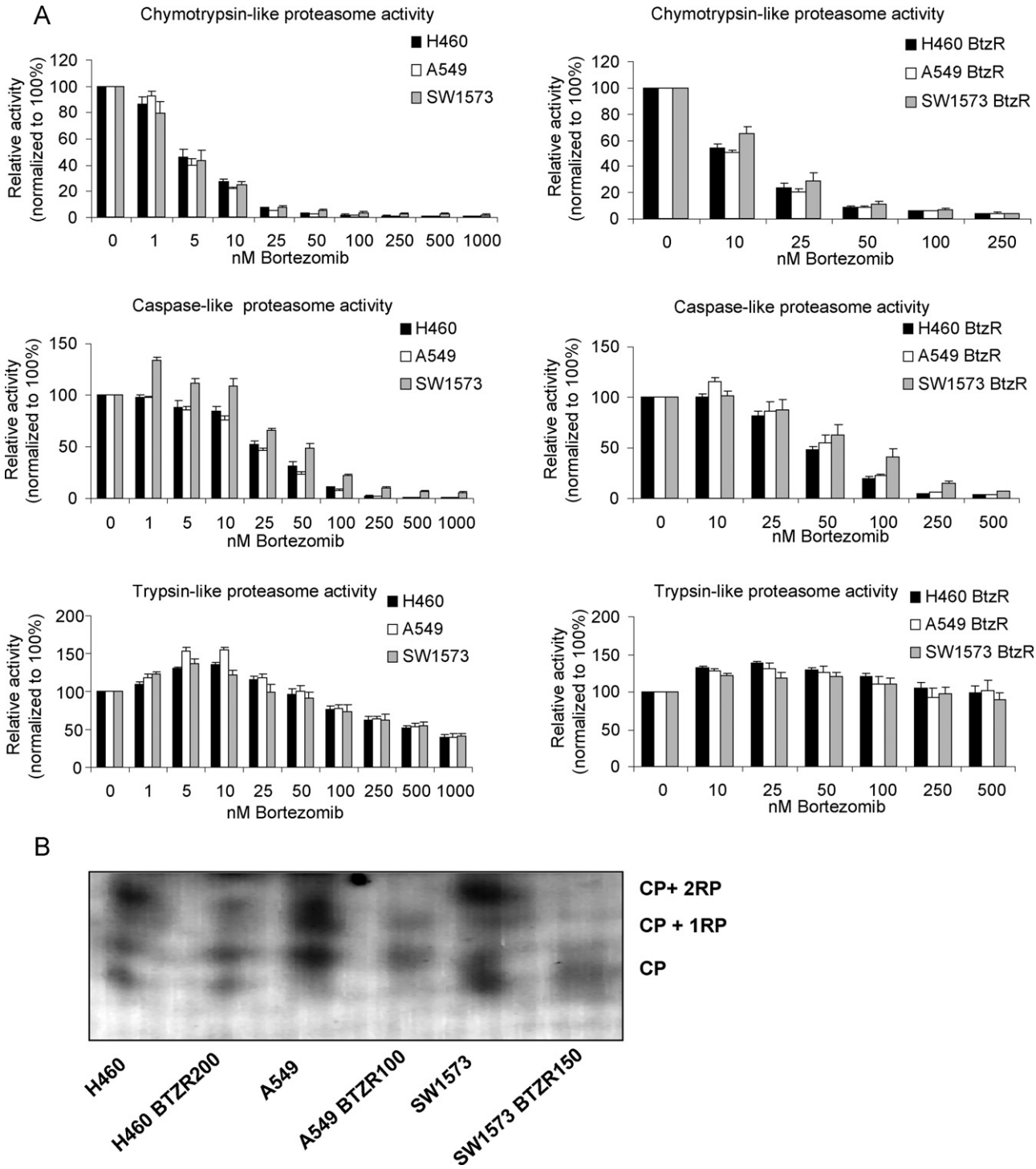

Fig. 4. Proteasome activities and proteasome inhibition in bortezomib resistant cells.
(A) Chymotrypsin-, caspase- and trypsin-like activities were determined using intact cells after incubation with a concentration range of bortezomib for 3 h. Proteasome activities were normalized to untreated cells which were set at 100%. Bortezomib resistant cells (right panel) required 2–2.5 fold higher bortezomib concentrations for comparable proteasome inhibition as the parental cells (left panel). Results represent the mean ± SEM of at least 3 experiments.
(B) Proteasome activity assay using native gel electrophoresis and suc-LLVY-amc substrate. CP: core particle, RP: regulatory particle.

caspase-like activities with IC_{80} values of 25–38 nM and 99–221 nM, respectively (Fig. 4A, right panel). Trypsin-like activity was not inhibited by bortezomib in these cells, even at high concentrations (500 nM). Similar to observations in parental cells, low bortezomib concentrations increased trypsin-like activity in bortezomib-resistant cells. Moreover, proteasome activity determined by native gel electrophoresis using the β5-subunit specific Suc-LLVY-amc substrate revealed strongly reduced proteasome activity levels in bortezomib-resistant derivatives, especially for $A549BTZR_{100}$ and $SW1573BTZR_{150}$ cells, when compared to parental cells (Fig. 4B). These findings suggest that basal proteasome activity levels cannot serve as predictors of acquired bortezomib-resistance. Altogether, these results demonstrate that in bortezomib-resistant cells, the proteasome can be inhibited by bortezomib, albeit at much higher concentrations than in the parental counterparts. Furthermore, despite increased levels of

Cell line	Type of mutation
H460	No mutation
H460 BTZR80	Ala49Thr
H460 BTZR200	Ala49Thr
A549	No mutation
A549 BTZR40	Met45Val
A549 BTZR100	Met45Val & Ala49Thr
SW1573	No mutation
SW1573 BTZR30	Cys52Phe
SW1573 BTZR150	Cys52Phe

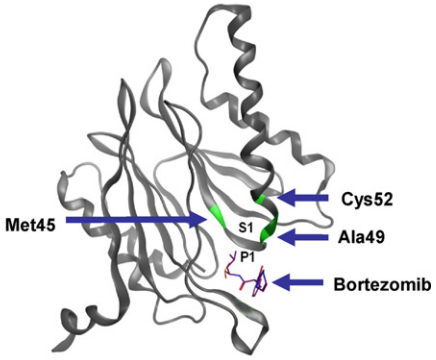

Fig. 5. Analysis of *PSMB5* gene mutation in bortezomib resistant cells.
Sequencing of the PSMB5 gene exon 2 revealed different mutations in bortezomib resistant cell lines. 3D-protein backbone structure of the proteasome β5-subunit (depicted in green) with the mutations detected in the resistant NSCLC cells. As a template, the 3D model includes the yeast proteasomal crystal structure in complex with Bortezomib and another proteasome inhibitor epoxomicin [52,54] and the bovine proteasomal crystal structure [55]. Abbreviations: P1: Substrate side chain 1, S1: Specificity binding pocket 1.

intact proteasome formation, proteasome activity is reduced in bortezomib-resistant cells.

3.6. Point mutations in PSMB5 in acquired bortezomib-resistant cells

Recently, three studies reported that bortezomib resistance in myeloid leukemia THP1 cells, multiple myeloma and T-cell leukemia Jurkat cells is associated with the emergence of mutations in exon 2 of the *PSMB5* gene encoding for the bortezomib drug-binding pocket of the β5-subunit [17–19]. Therefore, we performed DNA sequencing of *PSMB5* exon 2 in our panel of NSCLC cells and their bortezomib-resistant derivatives. In all cell lines studied, point mutations were identified, with each cell line displaying an apparent predominance for a specific mutation (Fig. 5). Interestingly, a second mutation was identified in A549BTZR$_{100}$ cells. In H460BTZR$_{80}$ and H460BTZR$_{200}$, a single G to A nucleotide shift was identified at the 322 position of *PSMB5*. This mutation introduced an Ala to Thr substitution at amino acid 49. In SW1573BTZR$_{30}$ and SW1573BTZR$_{150}$, a point mutation emerged leading to the substitution of a G to T nucleotide at the position 332 of *PSMB5* thereby converting Cys52 into Phe. In A549BTZR$_{40}$ and A549BTZR$_{100}$ cells, a single A to G nucleotide shift at the 310 position of *PSMB5* was identified that resulted in a substitution of amino acid Met45 to Val and an additional mutation, similar to the mutation found in H460BTZR cells, was identified in A549BTZR$_{100}$ cells. These latter mutations have also recently been identified in acquired bortezomib-resistant human CCRF-CEM leukemia cells and human multiple myeloma 8226 cells [42]. These results suggest that amino acid mutations in *PSMB5* likely play an important role in the acquisition of bortezomib resistance presumably via decreased bortezomib binding to the β5-subunit.

3.7. Cross-resistance of bortezomib-resistant cells to other PIs

We finally determined the cross-resistance of the bortezomib-resistant cells to a number of other PIs (Table 1). Bortezomib-resistant cells displayed a 2.8–20-fold resistance to MG132 which targets all β-subunits of the proteasome, and a 2.9–15-fold resistance to 4A6, a cytotoxic hexapeptide that specifically targets the β5-subunit of the proteasome [19]. Conversely, the proteasome inhibitor 5-amino-8-hydroxyquinoline (5AHQ) which targets the non-catalytic α7 subunit of the proteasome [32], showed no cross-resistance in bortezomib-resistant cells. Furthermore, recently developed irreversible proteasome inhibitors, such as ONX 0914 (formerly PR-957) specifically targeting the immuno-β-proteasome subunits, carfilzomib targeting the β5 and immuno-β5-subunit and an orally active derivative ONX 0912, were also studied. No cross-resistance was observed towards the immuno-proteasome inhibitor ONX 0914 in the H460-derived resistant cells, however in SW1573BTZR$_{150}$ and the A549-derived resistant cells a more than 2-fold and up to 13-fold (A549BTZR$_{100}$) increase in cross-resistance was detected, when compared to parental cells. Furthermore, A549BTZR cells and SW1573BTZR cells showed resistance towards carfilzomib ranging from 6.7 to 21.4-fold when compared to the parental cells. Interestingly, no appreciable levels of cross-resistance were observed in H460BTZR cells. Finally, we also examined cross-resistance towards ONX 0912. Strikingly high levels of cross-resistance were detected in A549BTZR$_{100}$ and SW1573BTZR$_{150}$ cells demonstrating even higher cross-resistance towards ONX 0912 than carfilzomib. These results demonstrate that cross-resistance occurs when bortezomib resistant cells are exposed to proteasome inhibitors targeting the β-subunits of the proteasome, which can be overcome by treatment with 5AHQ.

Beyond alterations at the proteasome target conferring bortezomib resistance and cross-resistance to other β5 targeted proteasome inhibitors, we also analyzed whether another mechanism may contribute to resistance. Drug extrusion via the multidrug efflux transporter P-glycoprotein (Pgp) has been shown to mediate a low level of bortezomib resistance [43–46]. However we found no cross-resistance to a prototypical Pgp substrate (i.e. doxorubicin) and differences in functional Pgp-activity between parental and Bortezomib-resistant cells (data not shown), suggesting that enhanced drug efflux via multidrug resistance transporters does not contribute to Bortezomib resistance in NSCLC cells.

4. Discussion

In the present study we found intrinsic bortezomib resistance in human NSCLC cell lines to correlate with high basal proteasome activity levels. On the other hand, acquired bortezomib resistance in H460, A549 and SW1573 cells was associated with over-expression of proteasome subunits and mutations in exon 2 of *PBSM5* gene leading to the requirement of higher bortezomib concentrations to inhibit the proteasomal activities. Although it is anticipated that this alteration constitutes the dominant mechanism of resistance in the NSCLC cell lines, we cannot rule out (minor) contributions of other factors to the resistant phenotype such as for example altered protein expression and degradation of specific apoptosis regulatory proteins. Intrinsic bortezomib sensitivity varied between the panel of NSCLC cells examined and low proteasome activities correlated with a high sensitivity to

Table 1
Cross resistance to different proteasome inhibitors.

	Bortezomib (nM)		Carfilzomib (nM)		MG132 (nM)		4A6 (μM)		ONX 0914 (nM)		ONX 0912 (nM)		5AHQ (μM)	
	IC_{50}	RF	IC_{50}	RF	IC_{50}	RF	IC_{50}	RF	IC_{50}	RF	IC_{50}	RF	IC_{50}	RF
H460	13 ± 2		13 ± 1.3		326 ± 45		2.7 ± 1.1		419 ± 69		110 ± 17		1.4 ± 0.3	
$H460BTZR_{80}$	173 ± 24	14	17 ± 4.7	1.3	869 ± 92	2.8	7.9 ± 1.1	2.9	460 ± 104	1.1	218 ± 4.8	2.0	1.7 ± 0.1	1.2
$H460BTZR_{200}$	276 ± 51	22	19 ± 6.8	1.5	1928 ± 71	5.9	7.3 ± 2.3	2.8	691 ± 61	1.6	1366 ± 322	12.4	0.9 ± 0.1	0.6
A549	8.7 ± 2		1.6 ± 0.3		137 ± 10		1.4 ± 0.3		174 ± 8.6		19 ± 3		1.6 ± 0.2	
$A549BTZR_{40}$	70 ± 9	8	13 ± 2.8	8.1	582 ± 60	4.3	4.6 ± 1.1	3.3	450 ± 63	2.6	187 ± 30	9.9	1.8 ± 0.3	1.1
$A549BTZR_{100}$	167 ± 16	19	34 ± 5.3	21	1412 ± 63	10.3	>15.6	>11	2242 ± 505	12.8	1050 ± 362	55.5	1.3 ± 0.1	0.8
SW1573	1.7 ± 0.4		2.1 ± 1.7		101 ± 1		1.1 ± 0.1		158 ± 30		17 ± 6.4		2.2 ± 0.2	
$SW1573BTZR_{50}$	30 ± 1.4	18	14 ± 3	6.7	864 ± 100	8.6	>10	>8.8	180 ± 12	1.1	229 ± 90	13.8	2.4 ± 0.6	1.1
$SW1573BTZR_{150}$	119 ± 28	70	26 ± 9	12	>2000	>19.8	>20	>14.6	504 ± 54	3.2	2071 ± 274	125	1.9 ± 0.3	0.8

IC_{50} values are the mean ± SEM of at least 3–7 experiments. Sensitivity to proteasome inhibitors was determined after continuous exposure for 72 h. RF = resistance factor (average IC_{50} values of bortezomib resistant cells/average IC_{50} values of the wild type cells).

bortezomib. It is likely that intrinsically low proteasome activities can be readily inhibited by low bortezomib concentrations, thereby resulting in proteasome activities below a threshold necessary for cell survival. Moreover, we demonstrated that NSCLC cells with acquired bortezomib-resistance show reduced basal proteasome activities when compared to their parental counterparts. This implies that basal proteasome activity is only an indicator of intrinsic bortezomib resistance and not of acquired bortezomib resistance. Further exploration of the molecular basis of acquired bortezomib resistance revealed a moderate overexpression (1.3–1.8 fold) of individual proteasome β-subunits in bortezomib-resistant cells. These findings are in line with previous studies where higher expression levels were reported in both bortezomib resistant cells [19,20,42,47] and bortezomib-adapted cells [48]. However, the increase in β-subunits expression is much lower than the 60-fold increase in THP1 leukemic acquired bortezomib resistant cells suggesting differences in the underlying mechanisms of resistance in NSCLC [19]. Interestingly, apart from a modest overexpression of the β-subunits and α7 subunit, we detected a marked overexpression of the immuno-β-subunits in the acquired resistant NSCLC cells. The immuno-proteasome is crucial for antigen processing and MHC class I antigen presentation, which is an essential mechanism for cells involved in the immune system [49]. However, knowledge on the immuno-proteasome and its inhibition in solid tumors is currently limited. Assembly of the immuno-proteasome was proposed to increase bortezomib sensitivity in several solid tumor cell lines [50]. In contrast, we found no cross-resistance towards immuno-proteasome inhibitor ONX 0914. Recently it was demonstrated that immuno-proteasomes were not only involved in antigen presentation but also play a key role in the maintenance of protein homeostasis by rapidly degrading oxidant-damaged proteins [51]. Since bortezomib is known to induce the accumulation of oxidized proteins, a key role for the enhanced expression levels of the immuno-proteasomes might be related to prevention of apoptosis. Clearly, the role of the immuno-proteasome subunits remains to be further elucidated.

Several mutations in the active site of the β5-subunit have been reported resulting in the conversion of Ala49Val, Ala50Val and Ala49Thr [17–20]. Consistently, transfection of a Ala49Thr-mutated *PBSM5* construct in KMS-11 MM cells reduced bortezomib-induced apoptosis by preventing accumulation of ubiquitinated proteins and fatal ER stress, but did not confer a similar resistance level as KMS-11 cells selected for bortezomib resistance following exposure to stepwise increasing concentrations [20]. Our findings reveal the same nucleotide 322 G to A shift in H460BTZR cells and $A549BTZR_{100}$ cells, but we also identified mutations at nucleotide position 332, resulting in Cys52Phe substitution in SW1573BTZR cells and at nucleotide position 310 substituting Met45Val in A549BTZR cells. These mutations have also been identified in bortezomib-resistant leukemic CCRF-CEM and 8226 cells [42]. Noteworthy, two mutations were detected in $A549BTZR_{100}$ cells. Elucidation of the crystal structure of the yeast 20S proteasome associated to bortezomib revealed the specificity and binding mode of bortezomib demonstrating that amino acids Met45 and Ala49 in the β5-subunit were essential for the binding of bortezomib [52] (see also Fig. 5). Bortezomib has been reported to induce a fit to Met45 thereby blocking β5-subunit mediated hydrolysis of hydrophobic peptide bonds [53]. Limited information is available regarding the role of Cys52 which we found here to be mutated in SW1573BTZR cells. Cys52 should not be directly involved in bortezomib binding, but rather resides in the S1 binding pocket of the β5 subunit [52]. It is likely that a mutation of Cys to the aromatic and bulky amino acid Phe will result in the physical obstruction of the bortezomib-binding pocket, thereby compromising bortezomib binding. Consistently, emerged

mutations should also result in decreased accessibility of natural proteins for degradation by the chymotrypsin activity, which may be reflected by the strongly reduced proteasome activity found in these cells. The presence of mutations in the β5-subunit of all generated acquired resistant cells strongly suggests that these genetic alterations are important for the development of high levels of bortezomib resistance.

In accordance to Groll et al., we observed a moderate stimulatory effect on trypsin-like proteasome activity in both wild type and bortezomib-resistant cells upon exposure to low concentrations (1–25 nM) of bortezomib (Fig. 4) [52]. In cells harbouring a mutation in the β5-subunit, we found that around 2.5 fold higher concentrations of bortezomib are able to induce similar levels of proteasome inhibition when compared to the parental cells (Fig. 4A). This is also reflected by approximately 5 fold higher levels of bortezomib required to obtain similar accumulation in poly-ubiquitinated proteins (Fig. 2B) or G2 arrest (Fig. 2C) indicating that other mechanisms contribute to bortezomib resistance as well. In this context we ruled out possible contributions by drug efflux transporters, but altered expression or degradation of apoptosis regulatory proteins deserves further consideration. We found that mitochondrial apoptosis regulatory proteins Mcl-1and NOXA, known proteasome substrates, were similarly expressed in H460 and SW1573 parental and resistant cells. Likewise, the expression of a number of additional apoptosis regulatory proteins was not altered, although a more extensive analysis of a wider range of proteins seems warranted. In contrast, A549BTZR$_{40}$ cells displayed higher basal levels of Mcl-1 and NOXA expression and a lack of further accumulation after bortezomib treatment. This may indicate that the β5 Met45Val mutation in these cells leads to substrate specific changes in protein degradation. Clearly, additional studies to the functional consequences of these different β5 mutations for protein degradation are required. On the other hand, we cannot exclude also other yet unidentified protein specific mechanisms have been changed in these bortezomib-adapted cells.

We found that the generated resistant NSCLC cells displayed cross-resistance to various other β-subunit targeting PIs including MG132, 4A6, Carfilzomib and ONX 0912, further emphasizing the relevance of β-subunit mutations in acquisition of bortezomib resistance. Interestingly and in line with this, bortezomib-resistant NSCLC cells did not display cross-resistance to the proteasome inhibitor 5AHQ that specifically targets the α7-subunit. A similar observation was reported by Li et al., demonstrating that 5AHQ was able to induce comparable levels of apoptosis in bortezomib-resistant THP1 cells and parental cells [32]. In addition, Li et al. also investigated K562 cells which express high basal levels of the β-5 subunit and proved to be bortezomib resistant which could be bypassed by 5AHQ. In mouse models of lung cancer initial responses to bortezomib were followed by the emergence of acquired resistance after prolonged treatment [30]. Whether in a similar way prolonged treatment of patients with bortezomib provokes acquired resistance/relapses associated with mutations in the β5 subunit awaits furhter exploration. In this situation the use of for example an α7 subunit inhibitor could provide an alternative treatment strategy. Together with our findings in NSCLC cells this indicates that 5AHQ may be a promising agent in overcoming bortezomib resistance in multiple tumor types.

One of the main questions concerning bortezomib sensitivity remains the distinct difference in response to bortezomib treatment between patients diagnosed with hematological or solid tumors. Possible differences in the functioning of the proteasome in these different cell types may be involved making further fundamental studies essential in order to better exploit the proteasome as a target in patients with solid tumors.

Acknowledgements

We thank Monette Aujay (Onyx Pharmaceuticals) for excellent technical assistance. Daan P. Geerke, Division of Molecular and Computational Toxicology, VU University is acknowledged for assistance with the 3D-modeling of PSMB5. We also thank Steven de Jong and Egbert Smit for their support. This project is supported by grant VU2006-3567 from the Dutch Cancer Society. YGA is a recipient of a visiting professor award from the Royal Netherlands Academy of Arts and Sciences (KNAW) and The Netherlands Organization for Scientific Research (NWO). Christopher Kirk has an ownership interest in Onyx Pharmaceuticals for >$10,000.

Appendix A. Supplementary data

Supplementary data associated with this article can be found, in the online version, at doi:10.1016/j.bcp.2011.10.009.

References

[1] Adams J. The proteasome: structure, function, and role in the cell. Cancer Treat Rev 2003;29(Suppl. 1):3–9.
[2] Voges D, Zwickl P, Baumeister W. The 26S proteasome: a molecular machine designed for controlled proteolysis. Annu Rev Biochem 1999;68:1015–68.
[3] Rock KL, Gramm C, Rothstein L, Clark K, Stein R, Dick L, et al. Inhibitors of the proteasome block the degradation of most cell proteins and the generation of peptides presented on MHC class I molecules. Cell 1994;78:761–71.
[4] Hershko A. Lessons from the discovery of the ubiquitin system. Trends Biochem Sci 1996;21:445–9.
[5] Adams J. The development of proteasome inhibitors as anticancer drugs. Cancer Cell 2004;5:417–21.
[6] Griffin TA, Nandi D, Cruz M, Fehling HJ, Kaer LV, Monaco JJ, et al. Immunoproteasome assembly: cooperative incorporation of interferon gamma (IFN-gamma)-inducible subunits. J Exp Med 1998;187:97–104.
[7] Altun M, Galardy PJ, Shringarpure R, Hideshima T, LeBlanc R, Anderson KC, et al. Effects of PS-341 on the activity and composition of proteasomes in multiple myeloma cells. Cancer Res 2005;65:7896–901.
[8] Crawford LJ, Walker B, Ovaa H, Chauhan D, Anderson KC, Morris TC, et al. Comparative selectivity and specificity of the proteasome inhibitors BzLLLCO-CHO, PS-341, and MG-132. Cancer Res 2006;66:6379–86.
[9] Orlowski RZ, Kuhn DJ. Proteasome inhibitors in cancer therapy: lessons from the first decade. Clin Cancer Res 2008;14:1649–57.
[10] Kuhn DJ, Chen Q, Voorhees PM, Strader JS, Shenk KD, Sun CM, et al. Potent activity of carfilzomib, a novel, irreversible inhibitor of the ubiquitin-proteasome pathway, against preclinical models of multiple myeloma. Blood 2007;110:3281–90.
[11] Demo SD, Kirk CJ, Aujay MA, Buchholz TJ, Dajee M, Ho MN, et al. Antitumor activity of PR-171, a novel irreversible inhibitor of the proteasome. Cancer Res 2007;67:6383–91.
[12] Zhou HJ, Aujay MA, Bennett MK, Dajee M, Demo SD, Fang Y, et al. Design and synthesis of an orally bioavailable and selective peptide epoxyketone proteasome inhibitor (PR-047). J Med Chem 2009;52:3028–38.
[13] Chauhan D, Singh AV, Aujay M, Kirk CJ, Bandi M, Ciccarelli B, et al. A novel orally active proteasome inhibitor ONX 0912 triggers in vitro and in vivo cytotoxicity in multiple myeloma. Blood 2010;116:4906–15.
[14] Cheriyath V, Jacobs BS, Hussein MA. Proteasome inhibitors in the clinical setting: benefits and strategies to overcome multiple myeloma resistance to proteasome inhibitors. Drugs R D 2007;8:1–12.
[15] McConkey DJ, Zhu K. Mechanisms of proteasome inhibitor action and resistance in cancer. Drug Resist Updat 2008;11:164–79.
[16] Chauhan D, Li G, Shringarpure R, Podar K, Ohtake Y, Hideshima T, et al. Blockade of Hsp27 overcomes bortezomib/proteasome inhibitor PS-341 resistance in lymphoma cells. Cancer Res 2003;63:6174–7.
[17] Lu S, Yang J, Song X, Gong S, Zhou H, Guo L, et al. Point mutation of the proteasome beta5 subunit gene is an important mechanism of bortezomib resistance in bortezomib-selected variants of Jurkat T cell lymphoblastic lymphoma/leukemia line. J Pharmacol Exp Ther 2008;326:423–31.
[18] Lu S, Yang J, Chen Z, Gong S, Zhou H, Xu X, et al. Different mutants of PSMB5 confer varying bortezomib resistance in T lymphoblastic lymphoma/leukemia cells derived from the Jurkat cell line. Exp Hematol 2009;37:831–7.
[19] Oerlemans R, Franke NE, Assaraf YG, Cloos J, van Zantwijk I, Berkers CR, et al. Molecular basis of bortezomib resistance: proteasome subunit beta5 (PSMB5) gene mutation and overexpression of PSMB5 protein. Blood 2008;112:2489–99.
[20] Ri M, Iida S, Nakashima T, Miyazaki H, Mori F, Ito A, et al. Bortezomib-resistant myeloma cell lines: a role for mutated PSMB5 in preventing the accumulation of unfolded proteins and fatal ER stress. Leukemia 2010;24:1506–12.
[21] Sterz J, von Metzler I, Hahne JC, Lamottke B, Rademacher J, Heider U, et al. The potential of proteasome inhibitors in cancer therapy. Expert Opin Investig Drugs 2008;17:879–95.

[22] Yang H, Zonder JA, Dou QP. Clinical development of novel proteasome inhibitors for cancer treatment. Expert Opin Investig Drugs 2009;18:957–71.
[23] Li T, Ho L, Piperdi B, Elrafei T, Camacho FJ, Rigas JR, et al. Phase II study of the proteasome inhibitor bortezomib (PS-341, Velcade) in chemotherapy-naive patients with advanced stage non-small cell lung cancer (NSCLC). Lung Cancer 2010;68:89–93.
[24] Davies AM, Ho C, Metzger AS, Beckett LA, Christensen S, Tanaka M, et al. Phase I study of two different schedules of bortezomib and pemetrexed in advanced solid tumors with emphasis on non-small cell lung cancer. J Thorac Oncol 2007;2:1112–6.
[25] Davies AM, Chansky K, Lara Jr PN, Gumerlock PH, Crowley J, Albain KS, et al. Bortezomib plus gemcitabine/carboplatin as first-line treatment of advanced non-small cell lung cancer: a phase II Southwest Oncology Group Study (S0339). J Thorac Oncol 2009;4:87–92.
[26] Fanucchi MP, Fossella FV, Belt R, Natale R, Fidias P, Carbone DP, et al. Randomized phase II study of bortezomib alone and bortezomib in combination with docetaxel in previously treated advanced non-small-cell lung cancer. J Clin Oncol 2006;24:5025–33.
[27] Lara Jr PN, Koczywas M, Quinn DI, Lenz HJ, Davies AM, Lau DH, et al. Bortezomib plus docetaxel in advanced non-small cell lung cancer and other solid tumors: a phase I California Cancer Consortium trial. J Thorac Oncol 2006;1:126–34.
[28] Voortman J, Smit EF, Honeywell R, Kuenen BC, Peters GJ, van de Velde H, et al. A parallel dose-escalation study of weekly and twice-weekly bortezomib in combination with gemcitabine and cisplatin in the first-line treatment of patients with advanced solid tumors. Clin Cancer Res 2007;13:3642–51.
[29] Ceresa C, Giovannetti E, Voortman J, Laan AC, Honeywell R, Giaccone G, et al. Bortezomib induces schedule-dependent modulation of gemcitabine pharmacokinetics and pharmacodynamics in non-small cell lung cancer and blood mononuclear cells. Mol Cancer Ther 2009;8:1026–36.
[30] Xue W, Meylan E, Oliver TG, Feldser DM, Winslow MM, Bronson R, et al. Response and resistance to NF-kB inhibitors in mouse models of lung adenocarcinoma. Cancer Discovery 2011. doi: 10.1158/2159-8290.CD-11-0073.
[31] de Jong MC, Slootstra JW, Scheffer GL, Schroeijers AB, Puijk WC, Dinkelberg R, et al. Peptide transport by the multidrug resistance protein MRP1. Cancer Res 2001;61:2552–7.
[32] Li X, Wood TE, Sprangers R, Jansen G, Franke NE, Mao X, et al. Effect of noncompetitive proteasome inhibition on bortezomib resistance. J Natl Cancer Inst 2010;102:1069–82.
[33] Muchamuel T, Basler M, Aujay MA, Suzuki E, Kalim KW, Lauer C, et al. A selective inhibitor of the immunoproteasome subunit LMP7 blocks cytokine production and attenuates progression of experimental arthritis. Nat Med 2009;15:781–7.
[34] Keepers YP, Pizao PE, Peters GJ, van Ark-Otte J, Winograd B, Pinedo HM. Comparison of the sulforhodamine B protein and tetrazolium (MTT) assays for in vitro chemosensitivity testing. Eur J Cancer 1991;27:897–900.
[35] Bijnsdorp IV, Kruyt FA, Gokoel S, Fukushima M, Peters GJ. Synergistic interaction between trifluorothymidine and docetaxel is sequence dependent. Cancer Sci 2008;99:2302–8.
[36] Bijnsdorp IV, Azijli K, Jansen EE, Wamelink MM, Jakobs C, Struys EA, et al. Accumulation of thymidine-derived sugars in thymidine phosphorylase overexpressing cells. Biochem Pharmacol 2010;80:786–92.
[37] Parlati F, Lee SJ, Aujay M, Suzuki E, Levitsky K, Lorens JB, et al. Carfilzomib can induce tumor cell death through selective inhibition of the chymotrypsin-like activity of the proteasome. Blood 2009;114:3439–47.
[38] Elsasser S, Schmidt M, Finley D. Characterization of the proteasome using native gel electrophoresis. Methods Enzymol 2005;398:353–63.
[39] Toornvliet R, van Berckel BN, Luurtsema G, Lubberink M, Geldof AA, Bosch TM, et al. Effect of age on functional P-glycoprotein in the blood-brain barrier measured by use of (R)-[(11)C]verapamil and positron emission tomography. Clin Pharmacol Ther 2006;79:540–8.
[40] van der Pol MA, Broxterman HJ, Pater JM, Feller N, van der Maas M, Weijers GW, et al. Function of the ABC transporters, P-glycoprotein, multidrug resistance protein and breast cancer resistance protein, in minimal residual disease in acute myeloid leukemia. Haematologica 2003;88:134–47.
[41] Voortman J, Checinska A, Giaccone G, Rodriguez JA, Kruyt FA. Bortezomib, but not cisplatin, induces mitochondria-dependent apoptosis accompanied by upregulation of noxa in the non-small cell lung cancer cell line NCI-H460. Mol Cancer Ther 2007;6:1046–53.
[42] Franke NE, Niewerth D, Assaraf YG, van Meerloo J, Vojtekova K, van Zantwijk CH, et al. Impaired bortezomib binding to mutant β5 subunit of the proteasome is the underlying basis for bortezomib resistance in leukemia cells. Leukemia; doi:10.1038/leu.2011.256.
[43] Lu S, Chen Z, Yang J, Chen L, Zhou H, Xu X, et al. The effects of proteasome inhibitor bortezomib on a P-gp positive leukemia cell line K562/A02. Int J Lab Hematol 2010;32:e123–31.
[44] Matsuki E, Miyakawa Y, Asakawa S, Tsukada Y, Yamada T, Yokoyama K, et al. Identification of loss of p16 expression and upregulation of MDR-1 as genetic events resulting from two novel chromosomal translocations found in a plasmablastic lymphoma of the uterus. Clin Cancer Res 2011;17:2101–9.
[45] Minderman H, Zhou Y, O'Loughlin KL, Baer MR. Bortezomib activity and in vitro interactions with anthracyclines and cytarabine in acute myeloid leukemia cells are independent of multidrug resistance mechanisms and p53 status. Cancer Chemother Pharmacol 2007;60:245–55.
[46] Rumpold H, Salvador C, Wolf AM, Tilg H, Gastl G, Wolf D. Knockdown of PgP resensitizes leukemic cells to proteasome inhibitors. Biochem Biophys Res Commun 2007;361:549–54.
[47] Liu Y, Liu X, Zhang T, Luna C, Liton PB, Gonzalez P. Cytoprotective effects of proteasome beta5 subunit overexpression in lens epithelial cells. Mol Vis 2007;13:31–8.
[48] Ruckrich T, Kraus M, Gogel J, Beck A, Ovaa H, Verdoes M, et al. Characterization of the ubiquitin-proteasome system in bortezomib-adapted cells. Leukemia 2009;23:1098–105.
[49] Rivett AJ, Hearn AR. Proteasome function in antigen presentation: immunoproteasome complexes, Peptide production, and interactions with viral proteins. Curr Protein Pept Sci 2004;5:153–61.
[50] Busse A, Kraus M, Na IK, Rietz A, Scheibenbogen C, Driessen C, et al. Sensitivity of tumor cells to proteasome inhibitors is associated with expression levels and composition of proteasome subunits. Cancer 2008;112:659–70.
[51] Seifert U, Bialy LP, Ebstein F, Bech-Otschir D, Voigt A, Schroter F, et al. Immunoproteasomes preserve protein homeostasis upon interferon-induced oxidative stress. Cell 2010;142:613–24.
[52] Groll M, Berkers CR, Ploegh HL, Ovaa H. Crystal structure of the boronic acid-based proteasome inhibitor bortezomib in complex with the yeast 20S proteasome. Structure 2006;14:451–6.
[53] Borissenko L, Groll M. 20S proteasome and its inhibitors: crystallographic knowledge for drug development. Chem Rev 2007;107:687–717.
[54] Groll M, Kim KB, Kairies N, Huber R, Crews CM. Crystal structure of epoxomicin: 20S proteasome reveals a molecular basis for selectivity of epoxyketone proteasome inhibitors. J Am Chem Soc 2000;122:1237–8.
[55] Unno M, Mizushima T, Morimoto Y, Tomisugi Y, Tanaka K, Yasuoka N, et al. The structure of the mammalian 20S proteasome at 2.75 Å resolution. Structure 2002;10:609–18.